Environmental Modelling and Software 137 (2021) 104972

Contents lists available at ScienceDirect

Environmental Modelling and Software

journal homepage: http://www.elsevier.com/locate/envsoft

QGIS-Landsat Indices plugin (Q-LIP): Tool for environmental indices computing using Landsat data

Boutaina Sebbah [a,*], Otmane Yazidi Alaoui [a], Miriam Wahbi [a], Mustapha Maâtouk [a], Nizar Ben Achhab [b]

[a] Geomatics and Land Management Research Unit, Faculty of Sciences and Techniques of Tangier, Abdelmalek Essaadi University, Tangier, Morocco
[b] Remote Sensing & GIS Research Unit, Abdelmalek Essaadi University, Tetuan, Morocco

ARTICLE INFO

Keywords:
Q-LIP
Landsat
QGIS
Environmental monitoring

ABSTRACT

Environmental monitoring has become of paramount importance for researchers and decision makers in order to better protect the environment and achieve sustainable development goals, especially with continuous population growth and rapid urbanization and industrialization processes that alter natural components of the environment and degrade the ecosystems. Hence, the use of Landsat data is of great significance, particularly in environmental monitoring and land management, due to their high spatial resolution and their free of cost availability since 1972. However, calculation of remotely sensed indices for environmental purpose occurs in several steps and requires minimum knowledge in imagery processing. This paper describes the development and design of Q-LIP "QGIS-Landsat Indices plugin"- a simple and easy-to-use tool to download, process and automatically calculate environmental indices from Landsat imagery. Q-LIP has been built under Python and designed as a QGIS software plugin; it is available to download from QGIS Plugin Repository.

Software availability

Name of software: : Q-LIP "Qgis-Landsat Indices plugin"
Developers: : Boutaina SEBBAH & Otmane YAZIDI ALAOUI
Contact information: : boutainasebbah@gmail.com
year first available: : 2020
Hardware required: : 8 GB RAM
Software required: : QGIS3.X
Software availability: : https://github.com/yazidiotmane/Q-LIP_QGIS
Software cost: : Free
Program language: : Python
Program size: : 623 KB on disk

1. Introduction

As the world population continues to develop, human activities continue their evolution too, and over-exploitation of biotic and abiotic resources become greater and greater, leading to a drastic degradation of environmental components and alteration of its natural characteristics. The need to understand and monitor environmental status and its spatiotemporal changes is of great significance in order to protect and manage natural resources efficiently, and therefore achieve sustainable development goals.

Ground-based techniques and in situ measurements have been traditionally used in environmental monitoring, but unfortunately, they have many limitations such as high cost and are not time or labour efficient. Moreover, they are only effective for small and limited regions, (Li et al., 2020). The use of remotely sensed data in environmental monitoring and ecological change-detection represents an effective surrogate of ground base methods (Xu et al., 2019), since it enables a large-scale area coverage and provides regular observations due to its diverse spatial and temporal resolution. Furthermore, it saves time and effort, and is cheaper compared to traditional methods. (De Araujo Barbosa et al., 2015).

Due to their free of cost availability, data acquired from Landsat sensors are considered as one of the most used data in global climate change researches, environmental monitoring and land management. Besides, they provide the longest-running and continuous time series intended for civil purposes since 1972 (NASA and USGS, 2018). Landsat data have been used in diverse fields in relation to environmental and ecological monitoring. It has been used in land and water surface temperature assessment (Ding and Elmore, 2015; Guo et al., 2016), in

* Corresponding author.
E-mail address: boutainasebbah@gmail.com (B. Sebbah).

https://doi.org/10.1016/j.envsoft.2021.104972
Accepted 12 January 2021
Available online 16 January 2021
1364-8152/

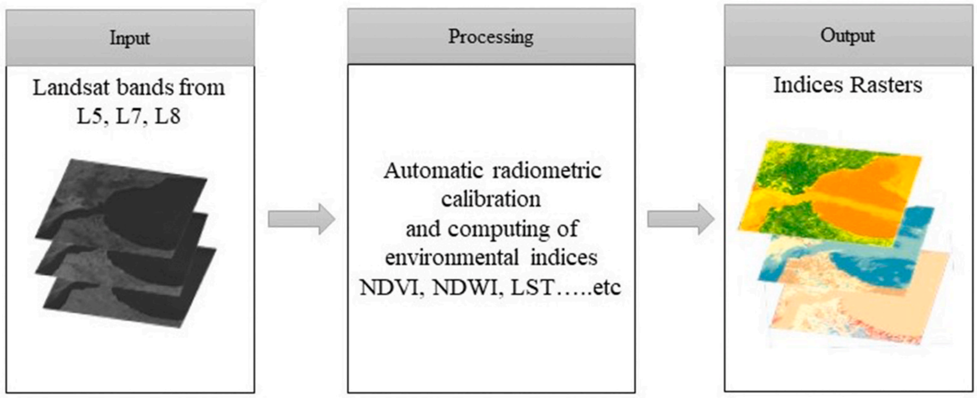

Fig. 1. Overview of Q-LIP functionalities.

vegetation cover changes and evapotranspiration estimation (Panda et al., 2019; Xie et al., 2019), in burn severity estimation and deforestation monitoring (Quintano et al., 2015; Schultz et al., 2016). They have also been used in urban studies as urban sprawl mapping (Sebbah et al., 2017a), and widely used in urban heat island studies, as they have a high-resolution thermal band compared to other existing data (Liu et al., 2020; Sebbah et al., 2017b). Quite often, these analyses are performed through different remote sensing indices that have been developed to assess and quantify environmental status as Normalized Difference Vegetation Index (NDVI) (Rouse et al., 1974), Normalized Difference Water Index (NDWI) (McFeeters, 1996), and Land surface Temperature (LST) (Jimenez-Munoz et al., 2014) … etc. Therefore, to calculate these multiple indices and produce variation maps, it is recommended to first preprocess Landsat images, as they are delivered in raw values, then calculate the required indices. This through-image processing software or even geographic information system software that have become commonly used, especially with the emergence of open access software such as QGIS. This has motivated us to develop Q-LIP "QGIS –Landsat indices plugin", presented in this paper, which is a plugin built under Python and openly available in QGIS to facilitate the processing and reduce its time, particularly for users without a strong background in image processing. This plugin is dedicated to download Landsat images with path 201 and raw 35 that includes the north of Morocco and the south of Spain on the Strait of Gibraltar and compute Landsat environmental indices in order to help researchers and decision makers to better understand and monitor environmental variation in this region. Q-LIP plugin also allows the calculation of Landsat environmental indices for any other area, provided that images are downloaded separately from existing online platforms.

2. Technical implementation

To facilitate Landsat environmental indices computing for a broad audience and for users without a strong knowledge in image processing, and to support the open-source model, Q-LIP plugin is integrated in QGIS (an open-source geographic information system software that permits the creation, visualization, editing and analysis of geospatial data). The use of QGIS is highly recommended since it is freely available, and its performance can be extended with a wide range of external plugins developed by its large community. Recently, many plugins have been developed under QGIS, to serve environmental purposes, such as evapotranspiration prediction (Ellsäßer et al., 2020), near surface air temperature mapping (Touati et al., 2020), climate change mitigation (Lindberg et al., 2018) and aquatic ecosystems evaluation (Nielsen et al.,

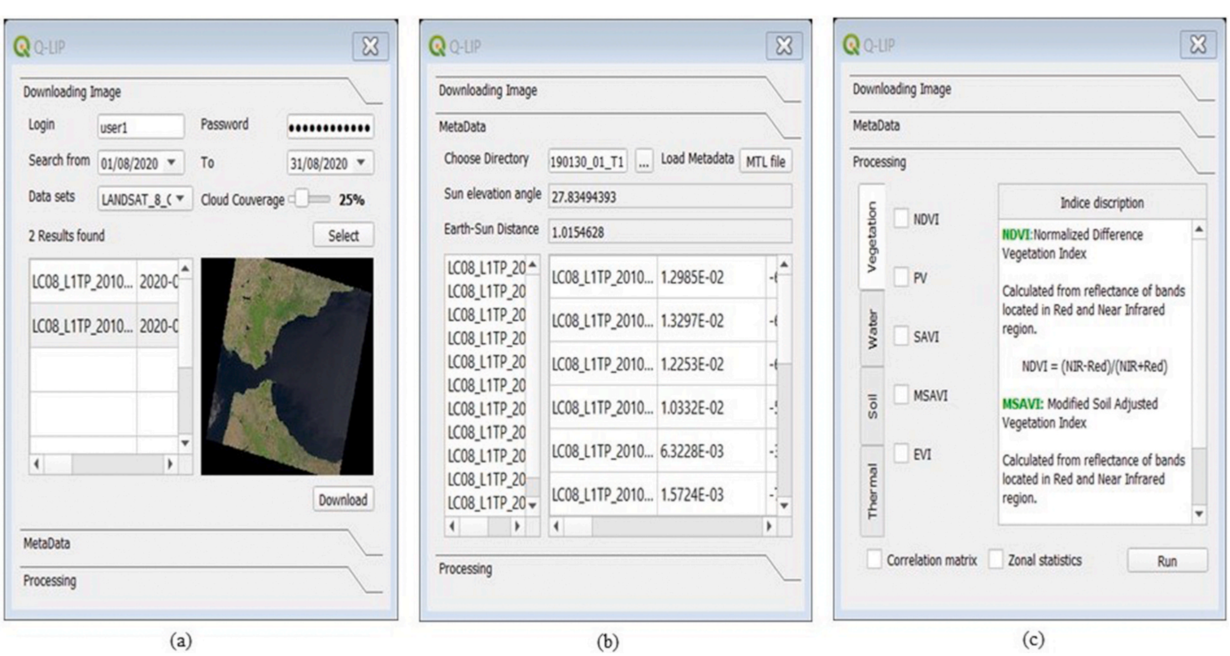

Fig. 2. The three tabs of Q-LIP graphical user interface, (a) Downloading image, (b) Metadata, (c) Processing.

2021). The core functionality of Q-LIP is written in Python (3.2) while the graphical user interface (GUI) is developed using Qt designer. Q-LIP is compatible with QGIS version (3.10) and all its functionalities can be run on a standard QGIS for desktop without requirements of any additional python libraries package. However, it performs hyper-complicated operations, requiring a minimum of 8 GB of RAM to compute all indices from Landsat images with more than 1 GB size.

Table 1
Environmental indices computed by Q-LIP plugin.

	Index	Formula	Reference
Vegetation indices	**NDVI**	$NDVI = \frac{NIR - RED}{NIR + RED}$	Rouse et al. (1974)
	PV	$PV = \left[\frac{NDVI - NDVI_{min}}{NDVI_{max} - NDVI_{min}}\right]^2$	Carlson and Ripley (1997)
	SAVI	$SAVI = \frac{NIR - RED}{NIR + RED + L} * (1 + L)$	Huete (1988)
	MSAVI	$(2 * NIR + 1 - sqrt((2 * NIR + 1)2 - 8 * (NIR - RED))) / 2$	Qi et al. (1994)
	EVI	$EVI = G * ((NIR - R) / (NIR + C1 * R - C2 * B + L))$	Huete et al. (2002)
Soil indices	**NDBI**	$NDBI = \frac{SWIR1 - NIR}{SWIR1 + NIR}$	Zha et al. (2003)
	LSE	$\varepsilon = \begin{cases} a + b\rho_{red} \\ \varepsilon_v PV + \varepsilon_s (1 - PV) + d\varepsilon \\ \varepsilon_v \end{cases}$	**L5 and L7** (Sobrino et al., 2008) **L8** Skoković et al. (2014)
	BI	$BI = \sqrt{RED^2 + NIR^2}$	Khan et al. (2001)
	BU	$BU = NDBI - NDVI$	He et al. (2010)
	NBR	$NBR = \frac{(NIR - SWIR2)}{(NIR + SWIR2)}$	García and Caselles (1991)
Water indices	**NDWI**	$NDWI = (B2 - B4)/(B2 + B4))$	McFeeters (1996)
	MNDWI	$MNDWI = (green - swir1)/(green + swir1)$	Xu (2006)
	NDMI	$NDMI = \frac{NIR - SWIR1}{NIR + SWIR1}$	Wilson and Sader (2002)
	AWEI	$AWEI_{nsh} = 4*(green - swir1) - (0,25 * NIR + 2,75 * swir2)$ $AWEI_{sh} = bleu + 2,5*green - 1,5*(NIR + swir1) - 0,25*swir2$	Feyisa et al. (2014)
Thermal indices	**LST**	$LST = \frac{BT}{\left\{1 + \left[\frac{\lambda \cdot BT}{\rho} \cdot \ln\varepsilon\right]\right\}}$	Artis and Carnahan (1982)
	UTFVI	$UTFVI = \frac{LST - LST_{mean}}{LST_{mean}}$	Zhang et al. (2006)

3. Process description

Using Landsat images from three different satellites (L5, L7 and L8), Q-LIP allows users to automatically compute some of the most utilized indices in environmental studies. The main tasks of this plugin can be summarized in three steps as illustrated in (Fig. 1).

1 . Download of Landsat images.
2 . Preprocess of Landsat images.
3 . Automatic computing of Landsat environmental indices

Q-LIP uses information from metadata file (MTL), included in the Landsat image folder, to extract necessary values for radiometric calibration, and then it calculates the chosen environmental indices. The output result is a raster layer with Tagged Image File Format (TIFF).

The GUI presented in (Fig. 2) will appear once the plugin is executed. Thus, the process is divided into three tabs: Downloading, Metadata and Environmental indices.

3.1. Downloading tab

The downloading tab allows the download of Landsat data with path 201 and row 35 from USGS Earth Explorer Platform. This image covers the north of Morocco and the south of Spain on the strait of Gibraltar. An account in USGS platform must be created in advance so that it can be used to download the required images directly from the plugin. Firstly, the users must enter their Login and Password, then choose date intervals (e.g. searching from 01/08/2020 to 31/08/2020). Secondly, the user should select the required satellite from the three available choices (Landsat 5, Landsat 7 or Landsat 8), and then specify the cloud coverage percentage. All found results will appear according to the criteria selected by the user and an overview of the image will appear once an image has been selected (Fig. 2a). Finally, the selected image can be downloaded.

3.2. Metadata tab

Metadata tab (Fig. 2b), allows navigation to the image directory, and loading the MTL file. Once the MTL is loaded, the needed information for preprocessing, such as sun elevation, earth-sun distance, radiance and reflectance multiplicative, additive scaling factors and Band specific thermal conversion constants (K1 and K2) will be loaded in the table. Radiometric calibration of Landsat images is performed automatically according to the following steps:

3.2.1. Conversion of DN to at-sensor spectral radiance

Conversion to at-sensor spectral radiance is an essential step to switch from raw digital numbers (DN) in Level 1 products to physical values (Chander et al., 2009). Conversion requires the knowledge of bands, specific rescaling gain and bias factors. The conversion of the DN from the three satellites was carried out with the following equations sited in (Chander et al., 2007; U.S. Geological Survey, 2019; USGS, 2011).

3.2.2. Conversion to TOA reflectance

Conversion from at-sensor spectral radiance to top of atmosphere (TOA) reflectance is an important step, especially in multi-temporal studies where data from multiple sensors are compared. This is so because it eliminates the cosine effect of different solar zenith angles generated by variability between data acquisitions time. It also compensates the various values of exo-atmospheric solar irradiance, resulting from variation of spectral bands as well as adjusting the difference in the Earth–Sun distance which arises due to differences between dates of data acquisition (Chander et al., 2009). TOA reflectance for the three sensors was computed according to equations cited in (Chander et al., 2009; U.S. Geological Survey, 2019).

3.2.3. Conversion to at-sensor brightness temperature

Spectral radiance of thermal bands from the three satellites (band 6, 6-2 and 10 of L5 TM, L7 ETM+ and L8 OLI/TIRS respectively) is converted to At-Satellite Brightness Temperature also known as effective at-satellite temperatures following equations in (Chander et al., 2009; U.S. Geological Survey, 2019). In this plugin, the use of thermal band 11 from L8 OLI/TIRS was avoided due to the large calibration uncertainty of this band mentioned by US Geological Survey (U.S. Geological Survey, 2019).

3.2.4. Environmental indices tab

The third tab is reserved for Landsat environmental indices (Fig. 2c), where the required indices to be computed must be checked. Indices are divided into four categories: vegetation, soil, water and thermal indices. Each category contains several indices, for example in "vegetation category" users can compute Normalized Difference Vegetation Index (NDVI), Portion of Vegetation (PV) and Modified Soil Adjusted Vegetation index (MSAVI). All indices proposed by Q-LIP plugin for each category and their formulas are summarized in Table 1. The

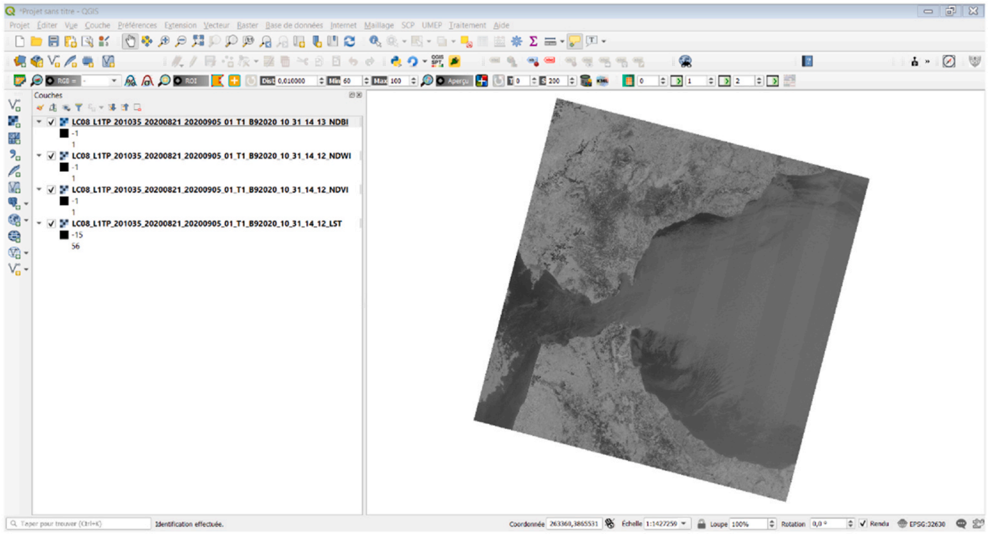

Fig. 3. Indices in QGIS Caneva after their calculation.

environmental indices tab also contains an index description table that gives information about proposed indices, their calculation formula, zonal statistics and correlation matrix between indices can also be extracted, and it is saved in TXT file.

4. Application and results

Q-LIP was tested using a computer with 8 GB of RAM. For example, the total processing time of a Landsat 8 image with 1.73 GB size is 3 min. For users working with multi-temporal Landsat data who desire to reduce processing time, it is recommended to use devices with 8 GB in RAM or more. Results of calculated indices are saved in the input image file, with the same name as input image, plus a suffix indicating index abbreviation and its date and processing time. Once the processing is completed, raster data of computed indices will appear in QGIS canvas (Fig. 3), allowing users to benefit from all QGIS functions and to modify raster proprieties or extract data, according to existing shape files. This facilitates the production of new maps and interprets them, depending on the user's objective. Indices computed by Q-LIP could be used in several environmental studies such as land cover change detection, burn severity, pre- and post-forest fire analyses, surface water detection for water resources management, Urban sprawls detection and in urban heat island delineation and assessment.

5. Conclusion

The present paper introduces Q-LIP "QGIS-Landsat Indices plugin", a simple and easy-to-use QGIS plugin built under Python allowing the automatic downloading, processing and computing of Landsat environmental indices. It permits the reduction of processing time to only 3 min for Landsat images with more than 1 GB size, when using computers with a minimum of 8 GB in RAM. Q-LIP can be a valuable tool for users without strong knowledge in remote sensing processing but are interested in environmental monitoring and land management.

Funding

This research did not receive any specific grant from funding agencies in the public, commercial, or not-for-profit sectors.

Declaration of competing interest

The authors declare that they have no known competing financial interests or personal relationships that could have appeared to influence the work reported in this paper.

Acknowledgments

The authors thank the insightful comments and suggestions from anonymous reviewers.

References

Artis, D.A., Carnahan, W.H., 1982. Survey of emissivity variability in thermography of urban areas. Remote Sens. Environ. 12, 313–329. https://doi.org/10.1016/0034-4257(82)90043-8.

Carlson, T.N., Ripley, D.A., 1997. On the relation between NDVI, fractional vegetation cover, and leaf area index. Remote Sens. Environ. 62, 241–252. https://doi.org/10.1016/S0034-4257(97)00104-1.

Chander, G., Markham, B.L., Barsi, J.A., 2007. Revised landsat-5 thematic mapper radiometric calibration. Geosci. Rem. Sens. Lett. IEEE 4. https://doi.org/10.1109/LGRS.2007.898285.

Chander, G., Markham, B.L., Helder, D.L., 2009. Summary of current radiometric calibration coefficients for Landsat MSS, TM, ETM+, and EO-1 ALI sensors. Remote Sens. Environ. 113, 893–903. https://doi.org/10.1016/j.rse.2009.01.007.

De Araujo Barbosa, C.C., Atkinson, P.M., Dearing, J.A., 2015. Remote sensing of ecosystem services: a systematic review. Ecol. Indicat. 52, 430–443. https://doi.org/10.1016/j.ecolind.2015.01.007.

Ding, H., Elmore, A.J., 2015. Spatio-temporal patterns in water surface temperature from Landsat time series data in the Chesapeake Bay. U.S.A. Remote Sens. Environ. 168, 335–348. https://doi.org/10.1016/j.rse.2015.07.009.

Ellsäßer, F., Röll, A., Stiegler, C., Hendrayanto, Hölscher, D., 2020. Introducing QWaterModel, a QGIS plugin for predicting evapotranspiration from land surface temperatures. Environ. Model. Software 130. https://doi.org/10.1016/j.envsoft.2020.104739.

Feyisa, G.L., Meilby, H., Fensholt, R., Proud, S.R., 2014. Automated Water Extraction Index: a new technique for surface water mapping using Landsat imagery. Remote Sens. Environ. 140, 23–35. https://doi.org/10.1016/j.rse.2013.08.029.

García, M.J.L., Caselles, V., 1991. Mapping burns and natural reforestation using thematic mapper data. Geocarto Int. 6, 31–37. https://doi.org/10.1080/10106049109354290.

Guo, G., Zhou, X., Wu, Z., Xiao, R., Chen, Y., 2016. Characterizing the impact of urban morphology heterogeneity on land surface temperature in Guangzhou, China. Environ. Model. Software 84, 427–439. https://doi.org/10.1016/j.envsoft.2016.06.021.

He, C., Shi, P., Xie, D., Zhao, Y., 2010. Improving the normalized difference built-up index to map urban built-up areas using a semiautomatic segmentation approach. Remote Sens. Lett. 1, 213–221. https://doi.org/10.1080/01431161.2010.481681.

Huete, A., Didan, K., Miura, T., Rodriguez, E.P., Gao, X., Ferreira, L.G., 2002. Overview of the radiometric and biophysical performance of the MODIS vegetation indices. Remote Sens. Environ. 83, 195–213. https://doi.org/10.1016/S0034-4257(02)00096-2.

Huete, A.R., 1988. A soil-adjusted vegetation index (SAVI). Remote Sens. Environ. 295–309.

Jimenez-Munoz, J.C., Sobrino, J.A., Skokovic, D., Mattar, C., Cristobal, J., 2014. Land surface temperature retrieval methods from landsat-8 thermal infrared sensor data.

Geosci. Rem. Sens. Lett. IEEE 11, 1840–1843. https://doi.org/10.1109/LGRS.2014.2312032.
Khan, N.M., Rastoskuev, V.V., Shalina, E.V., Sato, Y., 2001. Mapping salt-affected soils using remote sensing indicators - a simple approach with the use of GIS IDRISI. Ratio 5–9.
Li, J., Pei, Y., Zhao, S., Xiao, R., Sang, X., Zhang, C., 2020. A review of remote sensing for environmental monitoring in China. Rem. Sens. 12, 1–25. https://doi.org/10.3390/rs12071130.
Lindberg, F., Grimmond, C.S.B., Gabey, A., Huang, B., Kent, C.W., Sun, T., Theeuwes, N. E., Järvi, L., Ward, H.C., Capel-Timms, I., Chang, Y., Jonsson, P., Krave, N., Liu, D., Meyer, D., Olofson, K.F.G., Tan, J., Wästberg, D., Xue, L., Zhang, Z., 2018. Urban Multi-scale Environmental Predictor (UMEP): an integrated tool for city-based climate services. Environ. Model. Software 99, 70–87. https://doi.org/10.1016/j.envsoft.2017.09.020.
Liu, Y., Li, Q., Yang, L., Mu, K., Zhang, M., Liu, J., 2020. Urban heat island effects of various urban morphologies under regional climate conditions. Sci. Total Environ. 743 https://doi.org/10.1016/j.scitotenv.2020.140589.
McFeeters, S.K., 1996. The use of the Normalized Difference Water Index (NDWI) in the delineation of open water features. Int. J. Rem. Sens. 17, 1425–1432. https://doi.org/10.1080/01431169608948714.
NASA, USGS, 2018. Landsat - Benefiting Society for Fifty Years.
Nielsen, A., Schmidt Hu, F.R., Schnedler-Meyer, N.A., Bolding, K., Andersen, T.K., Trolle, D., 2021. Introducing QWET – a QGIS-plugin for application, evaluation and experimentation with the WET model: environmental Modelling and Software. Environ. Model. Software 135. https://doi.org/10.1016/j.envsoft.2020.104886.
Panda, S.S., Amatya, D.M., Muwamba, A., Chescheir, G., 2019. Estimation of evapotranspiration and its parameters for pine, switchgrass, and intercropping with remotely-sensed images based geospatial modeling. Environ. Model. Software 121, 104487. https://doi.org/10.1016/j.envsoft.2019.07.012.
Qi, J., Chehbouni, A., Huete, A.R., Kerr, Y.H., Sorooshian, S., 1994. A modified soil adjusted vegetation index. Remote Sens. Environ. 48, 119–126. https://doi.org/10.1016/0034-4257(94)90134-1.
Quintano, C., Fernández-Manso, A., Calvo, L., Marcos, E., Valbuena, L., 2015. Land surface temperature as potential indicator of burn severity in forest Mediterranean ecosystems. Int. J. Appl. Earth Obs. Geoinf. 36, 1–12. https://doi.org/10.1016/j.jag.2014.10.015.
Rouse, J.W.J., Haas, R.H., Schell, J.A., Deering, D.W., 1974. Monitoring vegetation systems in the great plains with erts. NASSP 351, 309.
Schultz, M., Clevers, J.G.P.W., Carter, S., Verbesselt, J., Avitabile, V., Quang, H.V., Herold, M., 2016. Performance of vegetation indices from Landsat time series in deforestation monitoring. Int. J. Appl. Earth Obs. Geoinf. 52, 318–327. https://doi.org/10.1016/j.jag.2016.06.020.
Sebbah, B., Wahbi, M., Maâtouk, M., 2017a. Analyse de l'étalement urbain de Tanger par le biais des données satellitaires (Landsat). In: 4ème Colloque de l'Association Francophone de Géographie Physique, p. 101.
Sebbah, B., Wahbi, M., Maâtouk, M., 2017b. Geographical information system tool monitoring the environmental impact of tangier industrial zones. Trans. Mach. Learn. Artif. Intell. 5 https://doi.org/10.14738/tmlai.54.3423.
Skoković, D., Sobrino, J.A., Jiménez-Muñoz, J.C., Sòria, G., Julien, Y., Mattar, C., Cristóbal, J., 2014. Calibration and Validation of Land Surface Temperature for Landsat8- TIRS Sensor. LPVE (L. Prod. Valid. Evol. ESA/ESRIN Frascati (Italy).
Sobrino, J.A., Jiménez-Muñoz, J.C., Sòria, G., Romaguera, M., Guanter, L., Moreno, J., Plaza, A., Martínez, P., 2008. Land surface emissivity retrieval from different VNIR and TIR sensors. In: IEEE Transactions on Geoscience and Remote Sensing, pp. 316–327. https://doi.org/10.1109/TGRS.2007.904834.
Touati, N., Gardes, T., Hidalgo, J., 2020. A GIS plugin to model the near surface air temperature from urban meteorological networks. Urban Clim 34, 100692. https://doi.org/10.1016/j.uclim.2020.100692.
U.S. Geological Survey, 2019. Landsat 8 (L8) Data Users Handbook Version 5.0.
Usgs, 2011. Landsat 7 science data users handbook landsat 7 science data users handbook. Natl. Aeronaut. Sp. Adm. 186.
Wilson, E.H., Sader, S.A., 2002. Detection of forest harvest type using multiple dates of Landsat TM imagery. Remote Sens. Environ. 80, 385–396. https://doi.org/10.1016/S0034-4257(01)00318-2.
Xie, Z., Phinn, S.R., Game, E.T., Pannell, D.J., Hobbs, R.J., Briggs, P.R., McDonald-Madden, E., 2019. Using Landsat observations (1988–2017) and Google Earth Engine to detect vegetation cover changes in rangelands - a first step towards identifying degraded lands for conservation. Remote Sens. Environ. 232, 111317. https://doi.org/10.1016/j.rse.2019.111317.
Xu, H., 2006. Modification of normalised difference water index (NDWI) to enhance open water features in remotely sensed imagery. Int. J. Rem. Sens. 27, 3025–3033. https://doi.org/10.1080/01431160600589179.
Xu, H., Wang, Y., Guan, H., Shi, T., Hu, X., 2019. Detecting ecological changes with a remote sensing based ecological index (RSEI) produced time series and change vector analysis. Rem. Sens. 11, 1–24. https://doi.org/10.3390/rs11202345.
Zha, Y., Gao, J., Ni, S., 2003. Use of normalized difference built-up index in automatically mapping urban areas from TM imagery. Int. J. Rem. Sens. 24, 583–594. https://doi.org/10.1080/01431160304987.
Zhang, Y., Yu, T., Gu, X., Zhang, Y., Chen, L.F., Yu, S.S., Zhang, W.J., Li, X.W., 2006. Land surface temperature retrieval from CBERS-02 IRMSS thermal infrared data and its applications in quantitative analysis of urban heat island effect. J. Remote Sens. 10, 789–797.